

2023-03

# Glass microbeads in coastal sediments as a proxy for traffic-related particulate contamination

Turner, A

<http://hdl.handle.net/10026.1/20347>

---

10.1016/j.marpolbul.2023.114663

Marine Pollution Bulletin

Elsevier BV

---

*All content in PEARL is protected by copyright law. Author manuscripts are made available in accordance with publisher policies. Please cite only the published version using the details provided on the item record or document. In the absence of an open licence (e.g. Creative Commons), permissions for further reuse of content should be sought from the publisher or author.*



# Glass microbeads in coastal sediments as a proxy for traffic-related particulate contamination

Andrew Turner<sup>\*</sup>, James Keene

School of Geography, Earth and Environmental Sciences, University of Plymouth, Plymouth PL4 8AA, UK

## ARTICLE INFO

### Keywords:

Road markings  
Urban  
Intertidal sediments  
Runoff  
Traffic dust proxies

## ABSTRACT

Retroreflective glass microbeads used in road markings have been characterised and subsequently identified in urban coastal sediments. Clear or translucent silica beads range in diameter from about 30 to 700  $\mu\text{m}$  and readily break from the matrix of detached or damaged markings on abrasion. At an urban location close to the city centre of Plymouth, southwest England, and in an estuary below a large road bridge, microbeads were detected in nearly all intertidal sediments analysed ( $n = 18$ ) and at concentrations up to about  $550 \text{ kg}^{-1} \text{ dw}$ . At a location not immediately impacted by major roads, beads were entirely absent from sediments ( $n = 9$ ). With a size range and density similar to silt-sand, glass beads appear to accumulate in sediment subject to road runoff and act as persistent proxies for traffic-related contamination. Although beads are unlikely to be inherently toxic, they may serve as indicators of more harmful chemicals in road dust.

## 1. Introduction

Coastal zone sediments act as a receptor of contaminants from a range of sources, including industries, waste water treatment, shipping, fishing, tourism, agriculture and road traffic (Sany et al., 2014; Christophoridis et al., 2019). One type of sediment contaminant that is associated with all of these sources and that has received increasing attention over the past decade is microplastics, including microrubbers (Peng et al., 2017; Yu et al., 2018; Leads and Weinstein, 2019; Tiwari et al., 2019). Microplastics are low density particles of  $<5 \text{ mm}$  in size that are typically isolated from sediment by flotation in a salt solution and subsequently identified and counted microscopically and spectroscopically (Woodall et al., 2014; Lutz et al., 2021).

In studies in which density separation is not considered, other forms of debris, including polymeric-based particles, have been detected that would otherwise remain neglected. For instance, Horton et al. (2017) identified road paints and plastiglomerates (plastic-mineral associations) in sediments from the River Thames catchment, while Turner (2019) found fragments of glazed ceramics in coastal sediments of Plymouth Sound. In a study of the Zuari Estuary, India, Shetye et al. (2019) detected clear to pale (yellow or grey) silica-based spherules of  $350 \mu\text{m}$  to  $1 \text{ mm}$  in diameter in three sediment samples that appeared to be glass retroreflective beads used in road markings. A subsequent study in the region of Kielce, central Poland, found that glass microbeads from road

markings were widely distributed in river sediments (Migaszewski et al., 2022).

In the present study, we characterise glass microbeads in samples of road markings collected from Plymouth, southwest England. Visual and physical characteristics are subsequently used to identify and count beads in coastal, intertidal sediment samples from three contrasting locations in the region. We address the potential for glass microbeads to act as a general proxy for traffic-related particulate contamination of the coastal zone and, more specifically, for harmful pigmented contaminants associated with road markings.

## 2. Methods

### 2.1. Road marking sampling and characterisation

Twenty samples of fragmented road paint (ten white and ten of varying shades of yellow; up to  $1 \text{ cm}$  in length and  $5 \text{ mm}$  in thickness) were taken by hand from the roadside throughout Plymouth where applications were visibly damaged or deteriorating. Samples were stored in individual specimen bags and in the dark until required for analysis.

A broad assessment of the elemental makeup of road markings was performed by energy-dispersive X-ray spectrometry according to Turner and Filella (2023). Briefly, samples were counted in a mining-soils mode

<sup>\*</sup> Corresponding author.

E-mail address: [aturner@plymouth.ac.uk](mailto:aturner@plymouth.ac.uk) (A. Turner).

for 60 s using a Niton XL3t 950 He GOLDD+ spectrometer (Niton-ThermoScientific) and concentrations of elements ( $Z > 19$ ) were computed from spectra via fundamental parameters with Niton Data Transfer software. The presence and nature of glass beads in the road marking samples were determined under a NIKON SMZ800 stereomicroscope (at up to  $63\times$  magnification) fitted with an Olympus SC30 camera and connected to Olympus Stream software. Beads were most clearly visible and distinguishable under LED ring-lighting; this minimised shadows and allowed light to be reflected back as distinctive, white circles. Samples were also examined under a JEOL JSM-6610 scanning electron microscope (SEM) outfitted with an Oxford Instruments energy-dispersive X-ray (EDX) spectrometer and AZtec software. The SEM was operated in low vacuum mode and used backscattered electron imaging with an accelerating voltage of 15 kV, a working distance of 10 to 15 mm and a magnification of  $300\times$ .

## 2.2. Sediment sampling

Intertidal sediment samples were taken from three contrasting locations around Plymouth with different proximities to and impacts from roads and stormwater discharges (Fig. 1).

Coxside is a semi-enclosed marina adjacent to a fishing harbour within 1 km of the city centre. The northern end of the harbour area receives runoff from the city centre via two strategic drainage corridors, with smaller stormwater discharges located throughout the region (Plymouth City Council, 2019). Coxside was sampled from a west-facing beach of gravel-mud-fine sand bordered by a slipway and a housing estate. On the Tamar Estuary, sampling took place from mudflats (silt to fine sand) on the east bank about 100 m downstream of a large road bridge located 5.5 km to the northwest of the city centre. Most runoff

from the bridge is discharged directly into the Tamar, with a small proportion diverted to an underground drainage system that is discharged into the estuary at sea level. The Plym Estuary was sampled from the mudflats (silt to fine sand) of Saltram, a country park around 4 km to the northeast of the city centre with no road access to the shore and no local stormwater discharges.

Samples were collected at low tide and during December 2021. At each location, and at distances of 5 m, 7.5 m and 10 m perpendicular to the waterline, a small trench was dug with a metal spade and sediment was retrieved from three depths (0–5 cm, 5–10 cm and 10–15 cm) using a metal spatula. Sediments were individually wrapped in aluminium foil and in the laboratory were transferred to a series of aluminium trays, covered with new foil, and dried at about  $30^\circ\text{C}$  for 24 h. Between about 20 and 40 g of each dried sample was then accurately weighed into a series of glass petri dishes, with any visible aggregates broken down with the aid of a metal spatula.

## 2.3. Identification and quantification of glass microbeads in sediment

Glass microbeads in dried but unprocessed intertidal sediment samples ( $n = 27$ ) were identified under the LED ring-lighting of the stereomicroscope (as described above). Beads were counted and sized with the aid of the polyline function and a 90-mm diameter, 1-cm gridded template placed under the petri dish. Specifically, with the aid of a 2-cm stainless steel probe, the sample was inspected in each grid from top to bottom in a zig-zag fashion, with material moved diagonally upwards and in the direction opposite to the viewing track in order to avoid double counting.

## 2.4. Identification and quantification of microbeads in sediment after flotation

After identifying and counting glass microbeads, sediment samples were subject to density separation in concentrated solutions of zinc chloride (250 mL of Fisher Scientific anhydrous  $\text{ZnCl}_2$  in distilled water; measured density =  $1.6\text{ g cm}^{-3}$ ) in a series of 300 mL, 25 cm high PVC columns. The contents were stirred with a glass rod before being allowed to settle for 24 h. Fifty mL of each solution was then decanted into a series of glass beakers, with a further 50 mL decanted after rinsing the remaining headspace of each column. The contents of each beaker were vacuum-filtered through Whatman 541 filters using a ceramic Bucher funnel before filters were oven-dried on watch glasses at  $30^\circ\text{C}$  for 24 h and beads were identified, sized and counted as above.

## 3. Results and discussion

### 3.1. Composition of road markings

Bulk analysis by XRF revealed that white road markings were dominated by Ca and Ti (concentrations  $> 10,000\text{ mg kg}^{-1}$ ), reflecting the use of calcite as a filler and titanium dioxide as a pigment, respectively. Yellow markings were dominated by Ca ( $> 10,000\text{ mg kg}^{-1}$ ) but Bi and V or Cr and Pb were present at relatively high concentrations in some cases ( $n = 2$  and  $n = 3$ , respectively), and as exemplified by the XRF spectra in Fig. 2. Here, the mass ratios of Bi to V (=4.8) and Pb to Cr (=4.2) are similar to those in bismuth vanadate (=4.1) and lead chromate (4.0), respectively, suggesting the use of these compounds to pigment the markings.

SEM-EDX analysis confirmed the presence of heterogeneously dispersed calcite and various pigmented particles in the road marking matrix. Glass microbeads were smooth, but with small and shallow (5  $\mu\text{m}$ ) grooves, etchings, pits and cavities, and particulate contaminants (up to 25  $\mu\text{m}$  in size) that had either adhered to or become embedded within the glass surface. In addition to silica, Ca, Mg and Na were present, indicative of soda-lime glass, along with traces of other elements that included Fe and Ti and that may be associated with components of



Fig. 1. Sampling locations for intertidal sediments in the vicinity of Plymouth, southwest England, with major roads shown in white.



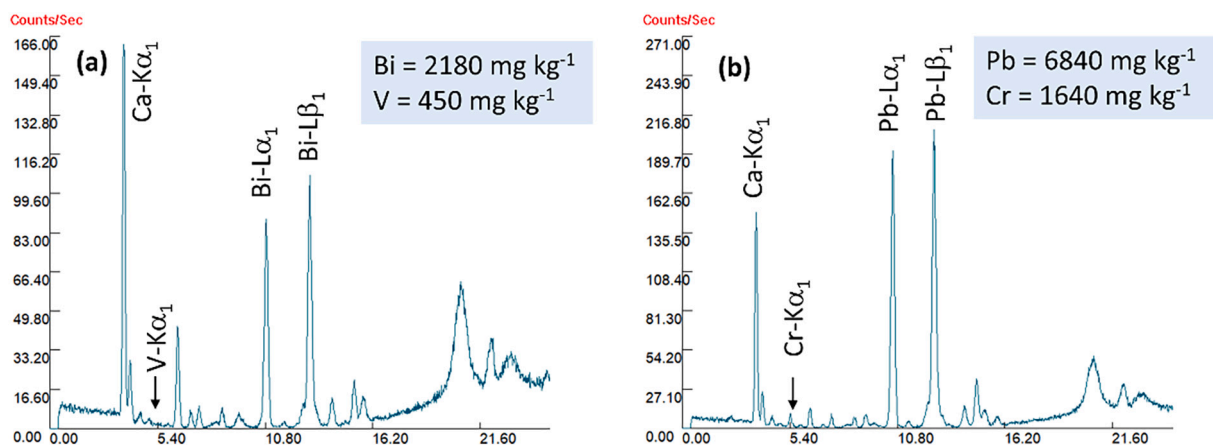


Fig. 2. XRF spectra (counts,  $s^{-1}$ , versus energy, keV) for (a) pale yellow and (b) dark yellow road markings. Annotated are concentrations of (a) Bi and V and (b) Pb and Cr. (For interpretation of the references to colour in this figure legend, the reader is referred to the web version of this article.)

the glass or particulate contaminants at its surface.

### 3.2. Distribution and abundance of glass microbeads in the road marking matrix

Fig. 3 shows examples of retroreflective glass microbeads embedded in various road markings observed under optical magnification. The surfaces of all white markings contained a dense and heterogeneous array of beads (up to about  $350 \text{ cm}^{-2}$ ) of varying diameter ( $\sim 50$  to  $500 \mu\text{m}$ ). Beads were highly rounded, with infrequent imperfections, and were mainly clear and transparent but occasionally darker and translucent. In some cases, beads were restricted to the surface, suggesting addition after the marking had been applied, while in others beads were evident throughout cross sections, suggesting pre-mixing of beads and marking before application. Glass microbeads were more difficult to identify in yellow markings because of lower contrasts and

the occurrence of additional and multi-coloured microscopic components that were embedded in the matrix or had been acquired from the road surface. Nevertheless, beads were less commonly observed in these markings and tended to be more widely dispersed and more uniform in size.

Lacking in our images of road markings were circular pits or holes where glass microbeads had been lost. Rather, it would appear that the marking matrix and beads are released concurrently as the surface is eroded. By crushing or gently filing samples with a metal spatula, the matrix tended to disaggregate, with beads mobilised relatively cleanly and with traces of the marking or partly encapsulated by fragments of the matrix (Fig. 4).

### 3.3. Glass microbeads in intertidal sediment

Fig. 5 exemplifies glass microbeads in unprocessed but dried

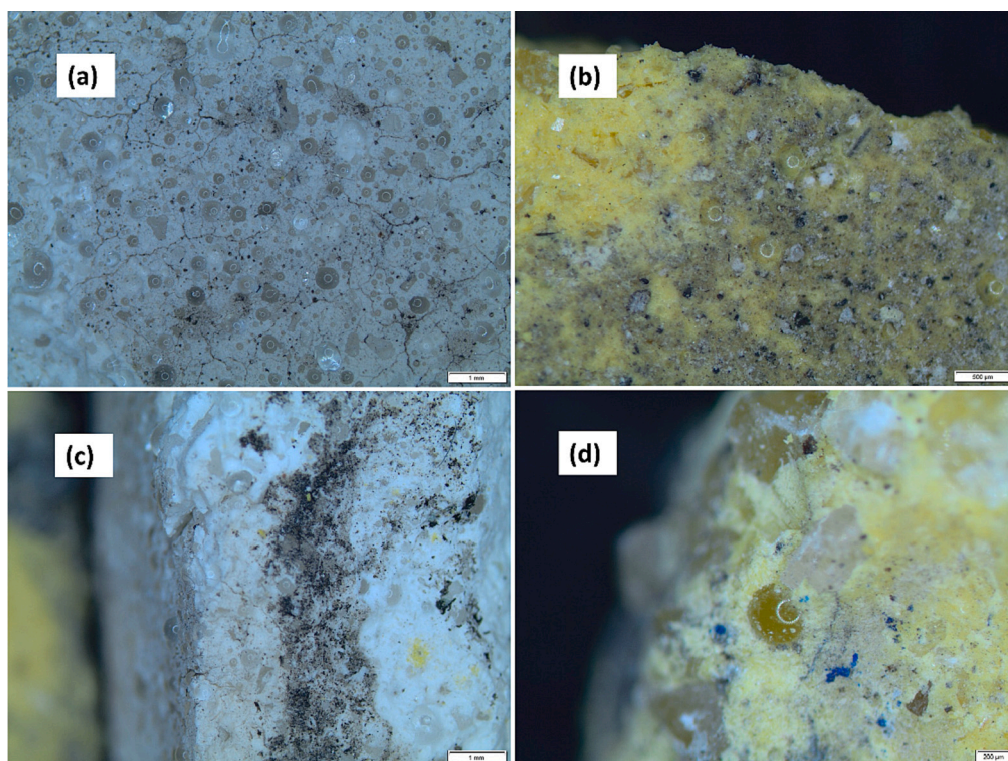
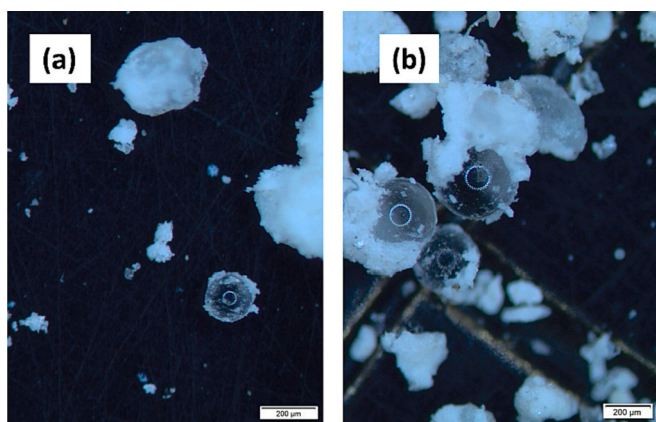


Fig. 3. Road markings observed under a stereomicroscope with glass microbeads exhibiting a distinctive white circle that reflects the ring lighting. (a) The heterogeneous distribution of beads at the surface of a white marking, (b) the distribution of clear beads at the surface of a yellow marking, (c) the distribution of beads through layers of white marking, and (d) a single bead embedded in yellow marking that appeared to be darker but on gentle crushing of the road marking matrix was transparent. (For interpretation of the references to colour in this figure legend, the reader is referred to the web version of this article.)



**Fig. 4.** (a) Glass microbeads released from a white road marking after gentle filing with a spatula. (a) A single bead with traces of the marking on the surface, and (b) beads partly encapsulated in fragments of the matrix.

intertidal sediment samples identified microscopically by their distinctive white, reflective circles and response to a metal probe. The majority were clear and transparent but occasional beads were dark, and while loose, surface deposits of sediment were always present, we found no clear evidence of residual road marking material. Median bead diameter was 160  $\mu\text{m}$ , with a range (30 to 690  $\mu\text{m}$ ) similar to that reported for beads associated with road markings above.

Table 1 shows the number of glass microbeads identified in the 27 unprocessed sediment samples (different perpendicular distances to low water mark and different depths at three locations) along with bead numbers normalised to the dry mass of sediment. Note that beads were never detected in samples that had been subsequently separated by flotation in  $\text{ZnCl}_2$  solution, indicating a density of  $>1.6 \text{ g cm}^{-3}$ . In total, 149 beads were counted, with numbers and concentrations in individual

samples ranging from 0 to 18 and 0 to 554  $\text{kg}^{-1} \text{ dw}$ , respectively. Amongst the locations, beads were detected in all samples from Tamar and in all but two samples from Coxside, but were absent at Saltram. At Coxside, the number and concentration of beads (but not size) increased with sediment depth at each perpendicular distance, suggesting a more important historical source, while at Tamar, beads were distributed with no clear depth dependence.

### 3.4. General discussion

Glass microbeads have a range of uses, from fillers in composites to abrasives in blasting of metal parts, as well as more specialised applications in various sectors, including agriculture, medicine and analytical sciences (Galuszka and Migaszewski, 2018). However, their widest and historically most important use, and in particular in the size range 100 to 1000  $\mu\text{m}$ , is in road markings for protection and retroreflectivity (Budov and Egorova, 1993).

Regarding the glass microbeads observed in coastal sediments in the present study, their sizes and visual characteristics, including lack of surface damage or fragmentation, suggest an origin associated with the degradation of road markings and transportation via road and storm-water runoff rather than local shot-blasting activities (Jacob et al., 2020). Moreover, discussions with Plymouth-based blast-cleaners and regional engineering specialists indicate that peening with glass beads is restricted to indoor use and that boat blasting normally involves glass fragments while the blasting of large structures, including a railway bridge over the Tamar Estuary, has employed grit.

Specifically, the microbeads reported here appear to be “standard”, solid, retroreflective beads dominated by amorphous silicon dioxide derived from recycled float glass and with a density of around  $2.5 \text{ g cm}^{-3}$ , a normative roundness in excess of 80 % and a maximum diameter of 850  $\mu\text{m}$  (Wenzel et al., 2022). These characteristics render glass microbeads similar to coarse silt to medium sand in terms of hydrodynamics, with calculated Stokesian settling velocities in coastal seawater

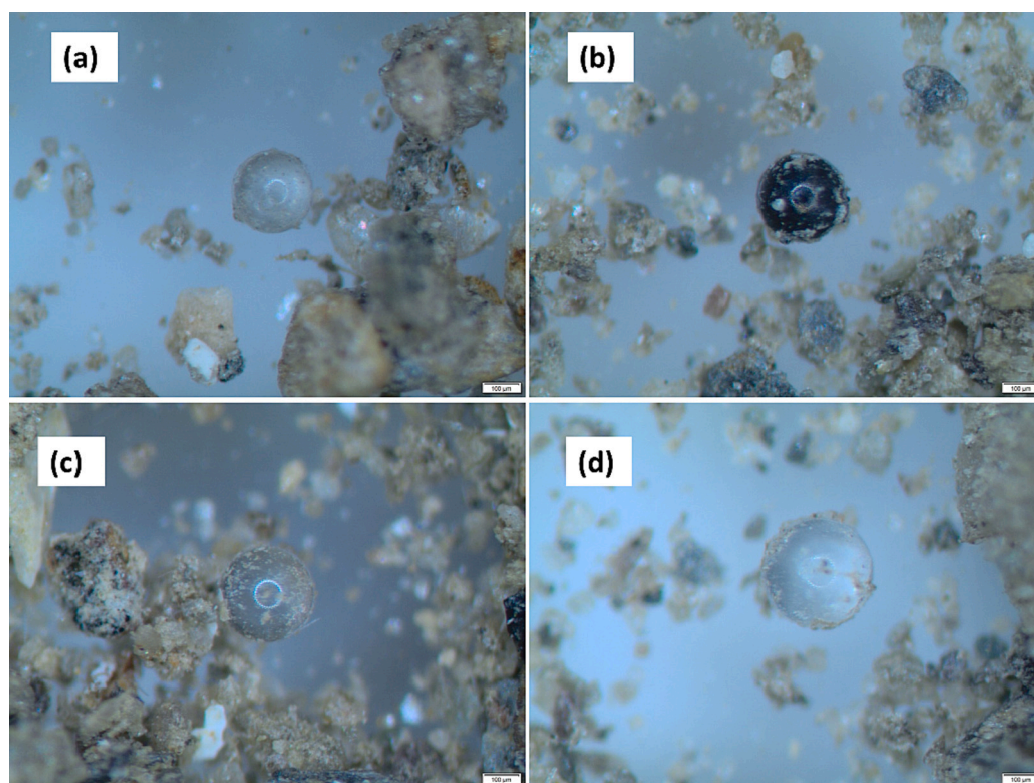


**Fig. 5.** Examples of glass microbeads in unprocessed but dried intertidal sediment identified under a stereomicroscope; (a) and (b) from Coxside, (c) and (d) from Tamar.



**Table 1**

Number of glass microbeads identified in each intertidal sediment sample and number of beads normalised to the dry mass of sediment. Perpendicular distance to the low water mark and depth of sampling are shown for the three locations.

Location	Distance, m	Depth, cm	No. beads	Beads, kg <sup>-1</sup> dw
Coxside	5	0–5	0	0
		5–10	14	401
		10–15	17	432
	7.5	0–5	1	35
		5–10	7	270
		10–15	9	307
	10	0–5	0	0
		5–10	2	56
		10–15	16	387
		(Total)	(66)	
Tamar	5	0–5	13	500
		5–10	2	62
		10–15	10	281
	7.5	0–5	18	554
		5–10	9	254
		10–15	9	317
	10	0–5	7	186
		5–10	5	146
		10–15	10	204
		(Total)	(83)	
Saltram	5	0–5	0	0
		5–10	0	0
		10–15	0	0
	7.5	0–5	0	0
		5–10	0	0
		10–15	0	0
	10	0–5	0	0
		5–10	0	0
		10–15	0	0
		(Total)	(0)	

(density = 1.02 g cm<sup>-3</sup>) ranging from about 0.1 to 40 cm s<sup>-1</sup> for the size range observed above. Presumably, therefore, beads eroded from road markings that enter the coastal zone primarily through road runoff and stormwater drainage subsequently disperse and accumulate with similarly-sized sediment grains. The presence of beads at locations close to a high density of urban streets, marked footways and stormwater streams (Coxside) and to a major road bridge (Tamar) but their absence at a location at least 300 m from any marked roads and relatively remote from significant stormwater discharges (Saltram) suggests that beads directly entering sediment accumulation zones with runoff are retained locally. However, it is also possible during dry periods that finer particles become airborne and are dispersed farther (Gałuszka and Migaszewski, 2018; Migaszewski et al., 2022).

Despite their widespread use in road markings, very little published information exists regarding the presence or concentration of glass microbeads in the environment. Specifically, beads have been described in road dusts from Venice, Italy (Zannoni et al., 2016), Tehran, Iran (Dehghani et al., 2017), Al Ain, Abu Dhabi (Habib et al., 2022) and Kielce, Poland (Migaszewski et al., 2022), and in sediments towards the mouth of the Zuari Estuary, India (Shetye et al., 2019) and throughout various rivers in the Kielce district (Migaszewski et al., 2022). The latter appears to be the only study to report glass microbeads on a concentration basis, with values greatest near to stormwater drains in the city centre (and up to 52,500 kg<sup>-1</sup> dw) and declining from about 5000 to 0 kg<sup>-1</sup> dw with increasing distance from the major road network (Migaszewski et al., 2022).

With so much recent interest in microplastics and microrubbers in aquatic sediments, and including those from urban settings (Wen et al., 2018; Liu et al., 2019; Yin et al., 2020; Lutz et al., 2021), lack of documentation of glass microbeads may seem surprising. However, plastics and rubbers are usually floated out of sediment samples in saline solutions before retrieval and identification, thereby leaving glass products in the discarded residues. While not as mobile as plastics and rubbers, the accumulation of glass beads may provide valuable semi-

quantitative information on areas impacted by road runoff and could be used in conjunction with microplastics and microrubbers for a more general evaluation of particulate contamination. Moreover, their chemical similarity to quartz and spheroidal shape means that beads could be preserved in the geological record for millions of years and act as a potential stratigraphic indicator of the Anthropocene (Gałuszka and Migaszewski, 2018; Irabien et al., 2020).

Glass microbeads could also serve as a more direct proxy for sediment contamination by paints and thermoplastics used in road markings. Thus, although Burghardt et al. (2022) suggest that the lack of road paints observed in sediment relates to the robustness or renewal of road markings, it is possible that paint is simply not distinguishable from other material, microscopically or otherwise, because of its propensity to fragment and abrade once detached from the road surface (see Fig. 3). Significantly, while beads themselves may not be inherently harmful (Dos Santos et al., 2013; Migaszewski et al., 2021), some of the metals that pigment road markings, like lead and chromium(VI), are highly toxic (Singh et al., 1999).

#### CRediT authorship contribution statement

AT: conceptualization; investigation; formal analysis; writing – original draft; writing – review and editing; project management.

JK: methodology; formal analysis; writing – original draft.

#### Declaration of competing interest

The authors declare that they have no known competing financial interests or personal relationships that could have appeared to influence the work reported in this paper.

#### Data availability

Data will be made available on request.

#### Acknowledgements

We are grateful to Dr Jodie Fisher and Mr Jamie Quinn (University of Plymouth) for technical support. The comments of two anonymous reviewers are greatly appreciated.

#### References

- Budov, V.V., Egorova, L.S., 1993. Glass microbeads, application, properties, and technology (review). *Glas. Ceram.* 50, 275–279.
- Burghardt, T.E., Pashkevich, A., Babić, D., Mosböck, H., Babčić, D., Żakowska, L., 2022. Microplastics and road markings: the role of glass beads and loss estimation. *Transp. Res. D* 102, 103123.
- Christophoridis, C., Bourliva, A., Evgenakis, E., Papadopoulou, L., Fytianos, K., 2019. Effects of anthropogenic activities on the levels of heavy metals in marine surface sediments of the Thessaloniki Bay, Northern Greece: spatial distribution, sources and contamination assessment. *Microchem. J.* 149, 104001.
- Dehghani, S., Moore, F., Akhbarizadeh, R., 2017. Microplastic pollution in deposited urban dust, Tehran metropolis, Iran. *Environ. Sci. Pollut. Res.* <https://doi.org/10.1007/s11356-017-9674-1>.
- Dos Santos, E.J., Herrmann, A.B., Prado, S.K., Fantin, E.B., dos Santos, V.W., De Oliveira, A.V.M., Curtius, J., 2013. Determination of toxic elements in glass beads used for pavement marking by ICP OES. *Microchem. J.* 108, 233–238.
- Gałuszka, A., Migaszewski, Z.M., 2018. Glass microspheres as a potential indicator of the Anthropocene: a first study in an urban environment. *The Holocene* 28, 323–329.
- Habib, R.Z., Ramachandran, T., Hamed, F., Al Kindi, R., Mourad, A.H.I., Thiemann, T., 2022. Microplastic in an arid region: identification, quantification and characterization on and alongside roads in an Ain, Abu Dhabi, United Arab Emirates. *J. Environ. Prot.* 13, 671–688.
- Horton, A.A., Svendsen, C., Williams, R.J., Spurgeon, D.J., Lahive, E., 2017. Large microplastic particles in sediments of tributaries of the River Thames, UK – abundance, sources and methods for effective quantification. *Mar. Pollut. Bull.* 114, 218–226.
- Irabien, M.J., Cearreta, A., Gómez-Arozamena, J., García-Artol, A., 2020. Holocene vs Anthropocene sedimentary records in a human-altered estuary: the Pasaia case (northern Spain). *Mar. Geol.* 429, 106292.

- Jacob, J., Thibault, A., Simonneau, A., Sabatier, L., Le Milbeau, C., Gautret, P., Ardito, L., Morio, C., 2020. High-resolution sedimentary record of anthropogenic deposits accumulated in a sewer decantation tank. *Anthropocene* 30, 100238.
- Leads, R.R., Weinstein, J.E., 2019. Occurrence of tire wear particles and other microplastics within the tributaries of the Charleston Harbor Estuary, South Carolina, USA. *Mar. Pollut. Bull.* 145, 569–582.
- Liu, F., Vianello, A., Vollertsen, J., 2019. Retention of microplastics in sediments of urban and highway stormwater retention ponds. *Environ. Pollut.* 255, 113335.
- Lutz, N., Fogarty, J., Rate, A., 2021. Accumulation and potential for transport of microplastics in stormwater drains into marine environments, Perth region, Western Australia. *Mar. Pollut. Bull.* 168, 112362.
- Migaszweski, Z.M., Gatuszka, A., Dołęgowska, S., Michalik, A., 2021. Glass microspheres in road dust of the city of Kielce (south-central Poland) as markers of traffic-related pollution. *J. Hazard. Mater.* 413, 125355.
- Migaszweski, Z.M., Gatuszka, A., Dołęgowska, S., Michalik, A., 2022. Abundance and fate of glass microspheres in river sediments and roadside soils: lessons from the Świętokrzyskie region case study (southcentral Poland). *Sci. Total Environ.* 821, 153410.
- Peng, G., Zhu, B., Yang, D., Su, L., Shi, H., Li, D., 2017. Microplastics in sediments of the Changjiang Estuary, China. *Environ. Pollut.* 225, 283–290.
- Plymouth City Council, 2019. Local Flood Risk Management Strategy. Protecting People, Places and Property: Local Flood Risk Management Strategy Part 2 - A Technical Design Guide Document, reference: EDG19/004/FRMS-02, Revision 2.
- Sany, S.B.T., Hashim, R., Salleh, A., Rezayi, M., Mehdinia, A., Safari, O., 2014. Polycyclic aromatic hydrocarbons in coastal sediment of Klang Strait, Malaysia: distribution pattern, risk assessment and sources. *PLoS ONE* 9, e94907.
- Shetye, S.S., Rudraswami, N.G., Nandakumar, K., Manjrekar, S., 2019. Anthropogenic spherules in Zuari estuary, south west coast of India. *Mar. Pollut. Bull.* 143, 1–5.
- Singh, J., Pritchard, D.E., Carlisle, D.L., Mclean, J.A., Montaser, A., Orenstein, J.M., Patierno, S.R., 1999. Internalization of carcinogenic lead chromate particles by cultured normal human lung epithelial cells: formation of intracellular lead-inclusion bodies and induction of apoptosis. *Toxicol. Appl. Pharmacol.* 161, 240–248.
- Tiwari, M., Rathod, T.D., Ajmal, P.Y., Bhangare, R.C., Sahu, S.K., 2019. Distribution and characterization of microplastics in beach sand from three different Indian coastal environments. *Mar. Pollut. Bull.* 140, 262–273.
- Turner, A., 2019. Lead pollution of coastal sediments by ceramic waste. *Mar. Pollut. Bull.* 138, 171–176.
- Turner, A., Filella, M., 2023. Lead and chromium in European road paints. *Environ. Pollut.* 316, 120492.
- Wen, X., Du, C., Xu, P., Zeng, G., Huang, D., Yin, L., Yin, Q., Hu, L., Wan, J., Zhang, J., Tan, S., Deng, R., 2018. Microplastic pollution in surface sediments of urban water areas in Changsha, China: abundance, composition, surface textures. *Mar. Pollut. Bull.* 136, 414–423.
- Wenzel, K.M., Burghardt, T.E., Pashkevich, A., Buckermann, W.A., 2022. Glass beads for road markings: surface damage and retroreflection decay study. *Appl. Sci.* 12, 2258.
- Woodall, L.C., Sanchez-Vidal, A., Canals, M., Paterson, G.L., Coppock, R., Sleight, V., Calafat, A., Rogers, A.D., Narayanaswamy, B.E., Thompson, R.C., 2014. The deep sea is a major sink for microplastic debris. *R. Soc. Open Sci.* 1, 140317.
- Yin, L., Wen, X., Du, C., Jiang, J., Wu, L., Zhang, Y., Hu, Z., Hu, S., Feng, Z., Zhou, Z., Long, Y., Gu, Q., 2020. Comparison of the abundance of microplastics between rural and urban areas: a case study from East Dongting Lake. *Chemosphere* 244, 125486.
- Yu, X., Ladewig, S., Bao, S., Toline, C.A., Whitmire, S., Chow, A.T., 2018. Occurrence and distribution of microplastics at selected coastal sites along the southeastern United States. *Sci. Total Environ.* 613–614, 298–305.
- Zannoni, D., Valotto, G., Visin, F., Rampazzo, G., 2016. Sources and distribution of tracer elements in road dust: the Venice mainland case of study. *J. Geochem. Explor.* 166, 64–72.